Fragmentation of clusters induced by collision with a solid surface: comparison of antimony and bismuth cluster ions

T.M. Bernhardt, B. Kaiser, K. Rademann

Walther-Nernst-Institut für Physikalische und Theoretische Chemie der Humboldt-Universität zu Berlin, Bunsenstrasse 1, D-10117 Berlin, Germany

Abstract. Mass-selected antimony cluster ions Sb_n^+ ($n = 3$–12) and bismuth cluster ions Bi_n^+ ($n = 3$–8) are allowed to collide with the surface of highly oriented pyrolytic graphite at energies up to 350 eV. The resulting fragment ions are analysed in a time-of-flight mass spectrometer. Two main fragmentation channels can be identified. At low impact energies both Sb_n^+ and Bi_n^+ cluster ions lose neutral tetramer and dimer units upon collision. Above about 150 eV impact energy Sb_3^+ becomes the predominant fragment ion of all investigated antimony clusters. The enhanced stability of these fragment clusters can be explained in the framework of the polyhedral skeletal electron pair theory. In contrast, Bi_n^+ cluster scattering leads to the formation of Bi_3^+, Bi_2^+ and Bi^+ with nearly equal abundances, if the collision energy exceeds 75 eV. The integral scattering yield is substantially higher in this case as compared to Sb_n^+ clusters.

PACS: : 33.15.Ta; 34.50.Dy; 36.40.Qv

Introduction

The understanding of the dynamical and energetical processes occurring during impact of metal clusters onto solid surfaces is important for thin film preparation via low energy cluster beam deposition methods as well as for the synthesis of new catalytic active materials consisting of adsorbed soft-landed clusters [1–5]. Cluster impact onto solid surfaces also opens a possibility to carry out chemical reactions under extreme temperature and pressure conditions [6, 7]. The energy dependence of fragment ion distributions generated by collision of a size-selected metal cluster with a solid surface gives information about cluster stability, cluster structure, fragmentation efficiency and energy transfer to the surface during collision. Surface scattering experiments at hyperthermal energies have been already performed with clusters consisting of non-conducting as well as semi-conducting elements [8–11]. In these cases the formation of stable fragment clusters is favoured. In contrast, surface collision induced dissociation of aluminium cluster anions is dominated by a stepwise loss of neutral atoms [12].

In this brief report, we present experimental results regarding the surface collision induced fragmentation of clusters consisting of semi-metallic elements. Time-of-flight mass spectrometry is used to record fragment ion abundance distributions of mass-selected positively charged antimony and bismuth clusters as a function of cluster size and impact energy.

Experimental

To investigate mass-selected metal cluster ions colliding with a solid surface we use a newly developed time-of-flight mass spectrometer arrangement which is schematically depicted in Fig. 1. In brief, it consists of a three stage molecular beam apparatus in which the cluster ions are directly generated in the expansion chamber by means of a modified pulsed arc cluster ion source [13, 14]. The cluster beam enters the second chamber through a skimmer and the ions are accelerated by combined acceleration and focusing fields into a Wiley-McLaren type time-of-flight mass spectrometer [15]. Scattering and detection takes place in the third chamber. A bunch of cluster ions with equal mass to charge ratio is selected via a specifically designed pulsed electrostatic mirror and deflected by $90°$ to a suitable substrate. The substrate is preceded by a deceleration lens to control the energy of the incoming ions and to focus them onto the substrate. The cluster ions hit the surface and the electrostatic field in front of the surface serves to reaccelerate the scattered ions into a second time-of-flight arrangement. The collision products pass the mirror, which is now grounded, and reach the microchannelplate detector. Signal registration and accumulation is performed by a fast waveform digitiser (LeCroy 9450). The electrostatic mirror can be rotated, in order to allow us to deflect the beam also either directly to the microchannelplate detector for mass-analysis, or into a reflectron for higher mass resolution (see Fig. 1). The impact energies assigned to the fragment ion spectra correspond to the mean impact energies of the colliding cluster ions. The energy spread is ± 40 to ± 100 eV. The surface employed in these investigations is the (0001) basal plane of highly oriented pyrolytic graphite (HOPG). The substrate is cleaved in air prior to its installation inside the vacuum chamber.
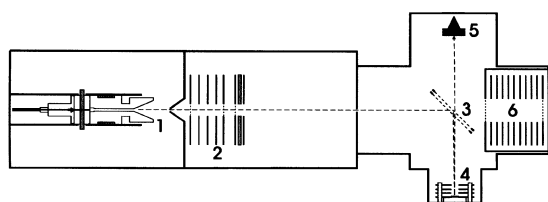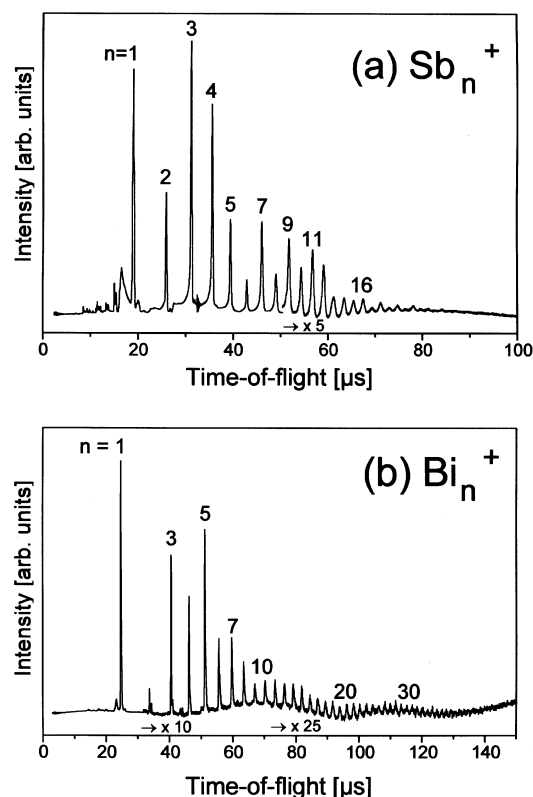
Fig. 1. Schematic drawing of the experimental setup: *1* cluster source, *2* acceleration and focusing, *3* rotatable electrostatic mirror, *4* scattering region (surface and preceding deceleration lens), *5* dual microchannelplate detector, *6* mass reflectron, the broken line gives the flight path of the ions in the scattering experiment
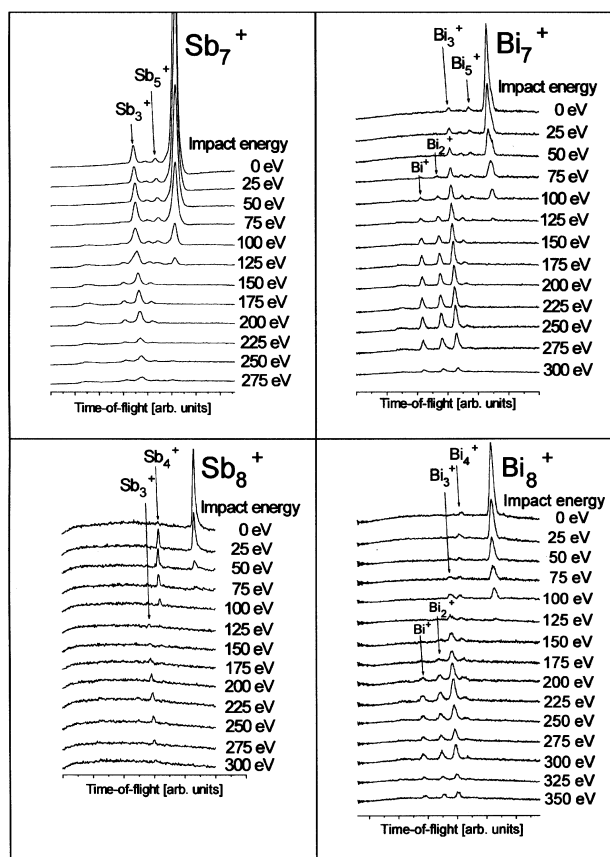
It is held at room temperature. The background pressure in the scattering region does not exceed 10^{-7} mbar during the experiments.

Results and discussion

Figure 2 shows mass spectra of positively charged antimony and bismuth clusters detected directly from the unscattered beam. The fragmentation mass spectra of X_n^+ clusters (X = Sb, Bi; $n = 7, 8$) are shown in Fig. 3 as a function of impact energy. It can be seen, that no continuous fragment ion distributions are observed, instead specific cluster peaks clearly dominate the spectra. In the case of Sb_8^+ and Bi_8^+ these are the tetramer and the trimer fragments. The abundances of these fragment ions are plotted in Fig. 4 as a function of impact energy. At low impact energies for both Sb_8^+ and Bi_8^+ the X_4^+ fragment predominates. This fragmen-

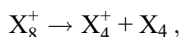**Fig. 3.** Fragmentation time-of-flight mass spectra for incident Sb_7^+, Bi_7^+, Sb_8^+ and Bi_8^+ cluster ions as a function of mean impact energy

Fig. 2a,b. Mass spectra sampled from the unscattered beam: **a** antimony cluster cations; **b** bismuth cluster cations

tation is supposed to correspond to the unimolecular lowest energy dissociation channel

$$X_8^+ \rightarrow X_4^+ + X_4 ,$$

which was also observed in photodissociation (PD) [16], collision induced dissociation (CID) [17], and delayed fragmentation experiments [18]. Bi_4 and especially Sb_4 are stable clusters, which is supported by the fact that they are present in the gas phase of the elements [19, 20]. The enhanced stability can be explained according to the predictions of the polyhedral skeletal electron pair theory (PSEPT) by the electronic structure of these clusters having an even number of valence electrons [21, 22]. Above a collision energy value of about 150 eV for Sb_8^+ and 75 eV for Bi_8^+ the X_3^+ fragment becomes most abundant. It can be supposed that in this energy regime multiple fragmentation takes place with the result that the most stable ionic fragment cluster is formed. The particular stability of the X_3^+ cluster ion was first inferred from mass-spectrometric studies of the intensity distributions of positively charged antimony and bismuth clusters from a laser vaporisation source [23]. A succinct explanation for this enhanced stability is also supplied by the PSEPT, which states a close relation between the electronic and the geometric structure of a series of homonuclear main group [24, 25] and transition metal clusters [26]. The theory predicts stability maxima for clusters with a specific number of valence electrons, namely of $2n+2$ (closo-Wade-cluster; n = number of atoms in the cluster), of $2n + 4$ (nido-Wade-cluster), and
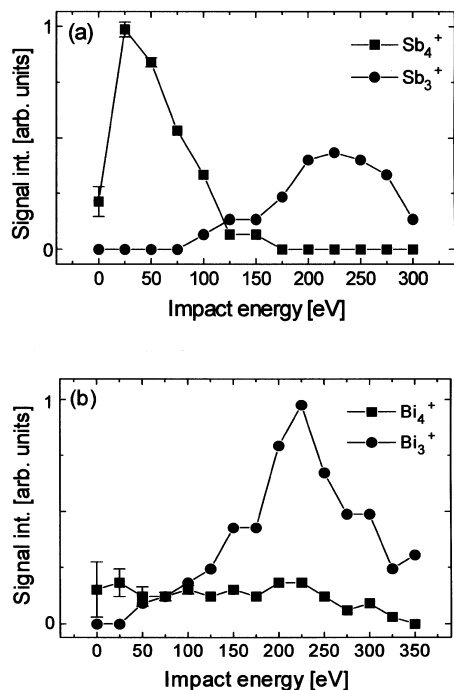
Fig. 4a,b. Intensities of the trimer and tetramer fragment ions for incident Sb_8^+ **a** and Bi_8^+ **b** clusters deduced from the corresponding mass spectra in Fig. 3. Error bars are drawn to account for the unknown amount of intact scattered cluster ions

Fig. 5a,b. Normalised fragment ion abundance patterns of all investigated incident cluster ions at two different mean impact energies: Sb_n^+: **a** 75 eV, **b** 275 eV; Bi_n^+: **a** 25 eV, **b** 225 eV

of $2n+6$ (arachno-Wade-cluster) electrons. The Sb_3^+ and Bi_3^+ clusters possess each eight valence electrons, hence the stable closo-structure can be assigned. Furthermore X_5^+ and X_7^+ are predicted to be of enhanced stability. This is supported by their pronounced appearance in the mass spectra of the unscattered beams of antimony and bismuth cluster cations (Fig. 2).

In Fig. 5 the fragment ion abundance patterns for all investigated clusters are summarised. The distributions shown in the part (a) of Fig. 5 correspond to the low energy scattering regime. Here the fragmentation spectra of the Bi_n^+ clusters are in their general features similar to those of Sb_n^+. The unimolecular loss of neutral tetramer units is characteristic for incident clusters X_n^+ with $n > 6$ in this energy range, as already stated above. Additionally a sequential loss of neutral X_2 units can be observed. For clusters with six and five atoms this is the predominant fragmentation channel. Sb_2 and Bi_2 are also stable species according to the PSEPT, and are present in the elemental vapours [19, 20]. For X_4^+ the loss of one atom to form the X_3^+ fragment is preferred. The part (b) of Fig. 5 reflects the typical fragmentation patterns resulting from the high energy impact of X_n^+. In the case of the investigated Sb_n^+ the closo-cluster Sb_3^+ is clearly the dominant fragment ion as predicted by the PSEPT. In contrast, Bi_n^+ clusters strongly fragment to form the complete fragment ion series Bi_3^+, Bi_2^+, and Bi^+, if the collision energy exceeds 75 eV. This cannot be understood in the framework of the PSEPT, because Bi_3^+ should also have a closo-structure with enhanced stability.

The proposed mechanism for the surface collision induced dissociation in the investigated energy range is ion activation by vibrational excitation [27]. Our results can be
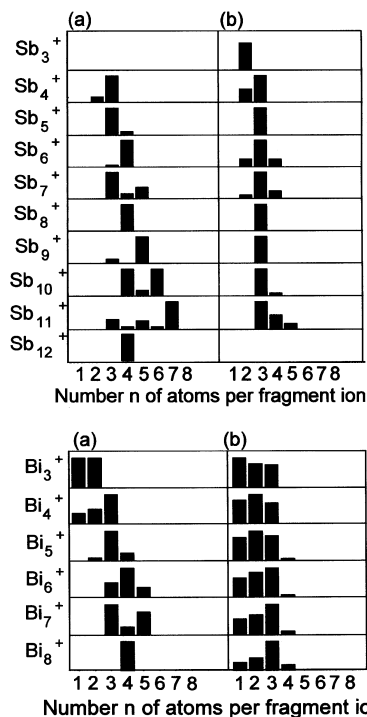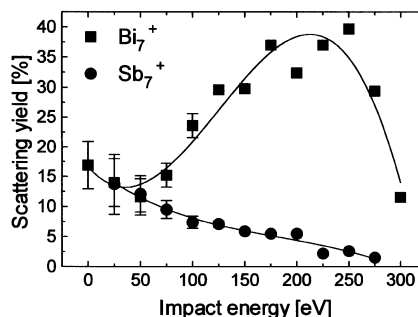

Fig. 6. Scattering yield plotted versus impact energy for the case of Sb_7^+ and Bi_7^+ collisions with graphite. The values are obtained from the corresponding total integrated signals in Fig. 3. The error bars reflect the uncertainty according to the unknown amount of intact scattered cluster ions

compared to low-energy CID measurements, because the fragmentation mechanism is also due to vibrational excitation and occurs on the ground state potential energy surface. Indeed, the lowest energy dissociation channels for Sb_n^+ ($n = 3–5$) and Bi_n^+ ($n = 3–14$) obtained by CID are in good agreement with our fragmentation data in the low energy regime [17].

An advantage of the surface induced dissociation technique over CID and PD techniques is the possibility to easily vary the collision energy. With increasing impact energy our data show fragmentation patterns for Sb_n^+ and Bi_n^+, which were not detected neither in the low-energy CID experiment, nor in high-energy CID [17] or PD (248 nm [16], 193 nm [18]) measurements.

There is a further interesting difference in the scattering behaviour of antimony and bismuth. We find a higher in-

tegral scattering yield for all Bi_n^+ clusters compared to the corresponding Sb_n^+ clusters at collision energies exceeding 75 eV. This is shown in Fig. 6 for the impact of X_7^+ clusters. At 200 eV collision energy the scattering yield integrated over all fragment ions is more than four times higher for Bi_7^+ than for Sb_7^+ clusters. Valence electron configuration arguments as supplied by the PSEPT are not sufficient to decide whether the stability of Sb_3^+ compared to Bi_3^+ could be the reason for the enhanced formation of Bi^+ and Bi_2^+ fragment ions as well as for the high overall scattering intensity for Bi_n^+ compared to Sb_n^+ clusters.

Conclusion

We have shown that the surface induced fragmentation of positive antimony and bismuth clusters leads at low impact energies to the same fragmentation patterns for clusters of the same size. The main fragmentation channel is the ejection of neutral tetramers and dimers. The low energy fragmentation mechanisms were explained by the stability of the formed neutral tetramers and dimers as predicted by the PSEPT.

This theory is also applicable to explain the stability of Sb_3^+, which is the predominant high energy impact fragment for antimony clusters. At collision energies exceeding a specific value, which is characteristic for the element, the fragment ion distributions and scattering yields of Sb_n^+ and Bi_n^+ clusters differ substantially. Scattering of bismuth clusters yields Bi_3^+, Bi_2^+ and Bi^+ with comparable abundances, but with a significant higher relative integral intensity. To understand the different fragmentation patterns of Bi_n^+ and Sb_n^+, more detailed informations about the cluster energetics and the dynamics of the cluster-surface collision process are needed.

References

1. Haberland, H. (Ed.): Clusters of Atoms and Molecules, vols. 1 and 2. Berlin: Springer 1994
2. Bower, J.E., Jarrold, M.F.: J. Chem. Phys. **97**, 8312 (1992)
3. Fuchs, G., Melinon, P., Santos Aires, F., Treilleux, M., Cabaud, B., Hoareau, A.: Phys. Rev. B **44**, 3926 (1991)
4. Cheng, H.-P., Landmann, U.: Science **260**, 1304 (1993)
5. Vandoni, G., Félix, C., Monot, R., Buttet, J., Harbich, W.: Chem. Phys. Lett. **229**, 51 (1994)
6. Cleveland, C.L., Landman, U.: Science **257**, 355 (1992)
7. Even, U., Schek, I., Jortner, J.: Chem. Phys. Lett. **202**, 303 (1993)
8. Whetten, R.L.: Acc. Chem. Res. **26**, 49 (1993)
9. St. John, P., Whetten, R.L.: Chem. Phys. Lett. **196**, 330 (1992)
10. Yeretzian, C., Beck, R.D., Whetten, R.L.: Int. J. Mass Spectrom. Ion Proc. **35**, 79 (1994)
11. Lill, T., Lacher, F., Busmann, H.-G., Hertl, I.-V.: Phys. Rev. Lett. **71**, 3383 (1993)
12. Terasaki, A., Tsukuda, T., Yasumatsu, H., Sugai, T., Kondow, T.: J. Chem. Phys. **104**, 1387 (1996)
13. Siekmann, H.R., Lüder, C., Faehrmann, J., Lutz, H.O., Meiwes-Broer, K.H.: Z. Phys. D **20**, 417 (1991)
14. Cha, C.-Y., Ganteför, G., Eberhardt, W.: Rev. Sci. Instrum. **63**, 5661 (1992)
15. Wiley, W.C., McLaren, I.H.: Rev. Sci Instrum. **26**, 1150 (1955)
16. Geusic, M.E., Freeman, R.R., Duncan, M.A.: J. Chem. Phys. **88**, 163 (1987)
17. Ross, M.M., McElvany, S.W.: J. Chem. Phys. **89**, 4821 (1988)
18. Brechignac, C., Cahuzac, P., Carlier, F., de Frutos, M., Leygnier, J., Roux, J.P.: J. Chem. Phys. **102**, 763 (1955)
19. Sattler, K., Mühlbach, J., Recknagel, E.: Phys. Rev. Lett **45**, 821 (1980)
20. Walstedt, R.E., Bell, R.F.: Phys. Rev. A **33**, 2830 (1986)
21. King, R.B., in: Jena, Pl, Rao, B.K., Khanna, S.N. (eds.): Physics and Chemistry of Small Clusters, Nato ASI Ser. B **158**, p. 79. New York: Plenum Press 1987
22. Mingos, D.M.P., Slee, T., Zhenyang, L.: Chem. Rev. **90**, 383 (1990)
23. Geusic, M.E., Freeman, R.R., Duncan, M.A.: J. Chem. Phys. **89**, 223 (1988)
24. Wade, K.: Adv. Inorg. Chem. Radiochem. **18**, 1 (1976)
25. Corbett, J.D.: Prog. Inorg. Chem. **21**, 129 (1976)
26. Fayet, P., McGlinchey, M.J., Wöste, L.: J. Am. Chem. Soc. **109**, 1733 (1987)
27. Cooks, R.G., Ast, T., Mabud, Md. A.: Int. J. Mass. Spectrom. Ion Proc. **100**, 209 (1990)